

Data Assimilation for Wildland Fires

Ensemble Kalman filters in coupled atmosphere-surface models

Jan Mandel, Jonathan D. Beezley, Janice L. Coen, and Minjeong Kim

Abstract

Two wildland fire models are described, one based on reaction-diffusion-convection partial differential equations, and one based on empirical fire spread by the level set method. The level set method model is coupled with the Weather Research and Forecasting (WRF) atmospheric model. The regularized and the morphing ensemble Kalman filter are used for data assimilation.

Index Terms

Weather Research and Forecasting model, WRF, wildfire modeling, wildland fire, level set method, reaction-diffusion systems, ensemble Kalman filter, morphing, registration, data assimilation, position correction, regularization, data assimilation, parallel computing

A wildland fire is a complex multiscale process affected by nonlinear scale-dependent interactions with other Earth processes. Physical processes contributing to the fire occur over a wide range of scales. While weather processes with characteristic scales ranging over 5 orders of magnitude from the several-hundred-km scale of large weather systems to the m-scale of small-scale effects and eddies, the chemical reactions associated with the thermal decomposition of fuel and combustion occur at scales of centimeters or less to produce flamelengths up to 60-m tall. Firelines travel with average speeds on the order of a fraction of a meter per second, while producing bursts of flame that travel at 50 meters per second, and chemical reactions occur on the order of seconds or less. The wind and buoyancy produced by the fire are among the extremes of atmospheric phenomena. Weather is the major factor that affects fire behavior, and two way interaction of weather and the atmosphere is essential – fires are known to dramatically influence the weather in their vicinity. The fire interacts with the atmosphere dynamics through fluxes of momentum, water vapor, and heat, and with the soil through moisture and heat retention.

Data does not come as exact coefficients and initial and boundary conditions. Instead, various quantities other than the model variables are measured at points spread over time and space, and the data are burdened with errors. Available data include fuel distribution maps, gridded atmospheric state from larger-scale weather models with assimilated weather data, point measurements from weather stations and fire sensors, two-dimensional airborne infrared imagery of the fire, and maps of fire extent produced by field personnel. The meteorological data is too sparse to resolve mesometeorological (2–20-km scale) features.

A computational model can capture only a select fraction of the significant mechanisms in the wildland fire process. Even if an accurate model existed, the data is not complete and accurate enough to make an accurate prediction possible. Also, one challenge of modeling is to estimate the probability that a forecast is accurate; a forecast has little value without additional information on what confidence level may be placed on it. So, it is natural to consider statistics based data assimilation methods. These methods include parameter and state estimation. Then the state of

the model is the probability distribution of possible wildfire scenarios. The data assimilation methods considered here proceed in analysis cycles. In each cycle, the model state is advanced in time, then new data is injected at the end of the cycle by combining the probability distribution of the state with data likelihood.

However, the strongly nonlinear character of fire causes difficulties for standard data assimilation methods [34], [42]. A fire is highly nonlinear and ignition is very sharp or even discontinuous on the model scale. Statistical variability in additive corrections to the state may cause spurious ignitions, and additive corrections are not adequate to make changes to the location of the fire. Probability distribution of the fire state can be multimodal and centered around the burning and not burning states at any given point in space. The whole fire state may concentrate around more than one distinct scenario, such as whether or not the fire jumps a road.

Classical data assimilation methods, such as statistical interpolation, 3DVAR, and 4DVAR [35] represent probability distributions only by the mean and the covariance. But only the normal distribution is completely determined by the mean and the covariance, so the strong non-Gaussian character of fire makes the use of those methods questionable. The complexities of the model and sharp nonlinearities rule out adjoint methods, such as 3DVAR and 4DVAR, which were developed for atmospheric models where the adjoint code can be produced by reversing the order of certain loops. Another option are ensemble methods. Although an ensemble can, in principle, represent a strongly non-Gaussian distribution, the EnKF [23] formulas are based on the assumption that the ensemble is a sample from a Gaussian distribution. Particle filters [19] also use an ensemble, and do not make the Gaussian assumption. However, particle filters are known to require a very large ensemble size, which grows fast for high-dimensional problems. This requirement makes them generally unsuitable for problems with more than a handful of variables, in particular for fire models, which have millions of gridpoints each of which in this solution method is a variable.

The goal of this article is to use nontraditional ensemble Kalman filter methods for the forecast of the behavior of wildland fires. The ultimate goal is to estimate the state of the fire from available data and deliver a short-term prediction faster than real time taking into account interactions between the fire and atmosphere. Although fire is a very complicated process, simple deterministic models that run fast can capture its essential behavior. Two such models are combined with improved versions of the EnKF. The *regularized EnKF* [34] incorporates an assumption that the physical fields are (mostly) smooth, thus helping to prevent large variations in temperature and spurious ignition. The *morphing EnKF* [5] exploits methods of image processing to combine spatial and amplitude corrections.

The work reported here is a part of an effort to build a Dynamic Data Driven Application System (DDDAS) for wildland fire prediction. The distinction between DDDAS and traditional control systems is that DDDAS is the dynamic streaming of data at runtime into the executing complex application, and in reverse the ability to dynamically steer the measurement process through this complex application model [17]. However, steering of the measurements is not considered here yet.

I. HOW TO MODEL WILDLAND FIRES?

In order to be faster than real time, fire models need to strike a balance between fidelity and fast execution. So, this article considers only two simplified 2D models for a fire in a layer just

above the ground. See “Wildland Fire Modeling” for related work.

A. Reaction-diffusion equations

Consider a model consisting a layer of fuel supply with concentration $F = F(x, t)$ (kg/m^2), $x = (x_1, x_2)$, and temperature $T = T(x, t)$ (K), which is assumed to burn at the relative rate $r(T)$ ($1/s$), dependent only on the temperature. The balance of heat in the fuel layer is described by the partial differential equation

$$c \frac{dT}{dt} = \nabla \cdot (k \nabla T) + (\vec{v} + \gamma \nabla z) \cdot \nabla T + \underbrace{AF r(T) - \overbrace{C(T - T_a)}^H}_{h(T)}, \quad (1)$$

where $\nabla = \left[\frac{d}{dx_1}, \frac{d}{dx_2} \right]$ is the gradient, \cdot is the dot product, c , k , A , and C are coefficients generally dependent on x and y , $\vec{v} = \vec{v}(x, t)$ is the wind speed, and $\gamma \nabla z$ is the correction for the gradient of the slope z (since fire moves faster uphill). The term $c \frac{dT}{dt}$ is the heat flux (J/m^2s) which is absorbed in the fuel and changes fuel layer's temperature. The diffusion term $\nabla \cdot (k \nabla T)$ models the heat transfer by short range radiation and air mixing, which causes the fire to spread between neighboring fuel particles (such as twigs and branches). The advection term $\vec{v} \cdot \nabla T$ is the heat flux due to wind. The external heat flux $h(T)$ consists of the heat flux $AF r(T)$, generated by burning the fuel, minus the heat flux

$$H = C(T - T_a), \quad (2)$$

escaping to the atmosphere at the ambient temperature T_a according to the Newton's law of cooling. The change in the fuel supply due to the burning is described by the fuel balance equation

$$\frac{dF}{dt} = -F r(T), \quad (3)$$

which is a collection of independent ordinary differential equations associated with the surface points (x, y) . The reaction rate is taken to be

$$r(T) = D e^{-B/(T - T_a)}, \quad (4)$$

where B and D are coefficients. The reaction rate (4) has the form of the Arrhenius reaction rate from chemical kinetics except for the offset T_a , which is to guarantee that the reaction rate is zero at the ambient temperature. Although the model (1)–(4) is simple, its solutions exhibit qualitative behaviors characteristic of combustion, known from chemical kinetics and theory of reaction-diffusion equations [28], [32].

Neglecting for the moment the change in the fuel supply F , there are three equilibria of the equation (1), given by the zeros of the function $h(T)$ (Fig. 2). The smallest zero is the ambient temperature, where there is no reaction and no heat flux to the atmosphere. This smallest zero is a stable equilibrium because the derivative $h'(T_a) < 0$. The middle zero is the ignition temperature T_i , which is an unstable equilibrium, $h'(T_i) > 0$. At the ignition temperature, the heat generated by the reaction balances the heat escaping to the atmosphere, but a small increase of the temperature above T_i creates a positive heat flux, which increases the temperature further,

thus leading to the development of fire. The temperature climbs toward the largest zero of h , but then it decreases as the fuel burns off following (3).

Solutions of the system (1)–(4) exhibit propagating combustion waves, at least for coefficients in certain ranges. At the leading edge of the combustion wave, the diffusion term spreads the heat into not yet ignited fuel and increases its temperature. Once the temperature is high enough for the heat generated by the reaction to overcome the heat loss, the fuel ignites and the temperature increases very quickly. The fuel then burns off and cools down, creating the trailing edge of the combustion wave. As a result, the combustion wave moves into yet unburned fuel and leaves behind fuel burned down to a quantity no longer sufficient to sustain the reaction.

Unfortunately, taking coefficients from data and expecting to get the correct combustion wave speed is hopeless. The reason is that coefficients are a homogenized form of unknown microscale data and many important physical processes are not modeled at all. For example, the model ignores the effect of the disappearance of fuel on the total heat capacity c of the fuel layer, storage of the heat in the ground, the chemical kinetics of intermediate products of combustion, the fine scale fire dynamics on the surface and in the interior of the wood, and evaporation of moisture. Fortunately, suitable coefficients can be identified from observed macroscopic behavior of the fire. In [42], the coefficients were determined from temperature profile measured by a stationary sensor passed over by a moving combustion wave, and from the measured speed of the combustion wave (Fig. 1). Combustion wave speed is also called the fire spread rate.

The model (1)–(4) can be discretized by standard finite difference techniques, with a sufficiently fine mesh to resolve the ignition region and unwinding of the advection term for stability. In the computations reported in [42], this discretization requires a mesh with cell size $2m$ or less and time step $1s$ or less.

B. Fireline curve propagation

An empirical fire propagation model imposes the fire spread rate directly, replaces the leading edge of the combustion wave by instantaneous ignition, and replaces the fuel depletion rate by an imposed one.

Consider fire burning in the area $\Omega = \Omega(t)$ with the boundary $\Gamma = \Gamma(t)$, called the fireline, with outside normal $\vec{n} = \vec{n}(x, t)$, $x \in \Gamma(t)$. The time of ignition $t_i(x)$ at a point $x \in \Omega(t)$ is defined as the time when the point is at the fireline, $x \in \Gamma(t_i(x))$.

The model postulates that the fireline evolves with a given spread rate $S = S(x, t)$ in the normal direction. The spread rate is of the form [51], [10]

$$S = \begin{cases} 0, & \text{if } \tilde{S} < 0, \\ S_{\max}, & \text{if } \tilde{S} > S_{\max}, \\ \tilde{S}, & \text{otherwise,} \end{cases} \quad \tilde{S} = c_0 + \phi_W + \phi_S R_0, \quad \phi_W = a(\vec{v} \cdot \vec{n})^b, \quad \phi_S = d \nabla z \cdot \vec{n}, \quad (5)$$

where R_0 is the spread rate in the absence of wind, $c_0 = 0$ or 1 , ϕ_W is the wind correction, $\vec{v} \cdot \vec{n}$ is the component of the wind \vec{v} in the spread direction \vec{n} , ϕ_S is the terrain correction, and $\nabla z \cdot \vec{n}$ is the slope of the terrain z in the spread direction \vec{n} .

In the burning area, the model postulates that the fuel decreases exponentially from ignition time

$$F(x, t) = \begin{cases} F_0(x) e^{-(t-t_i(x))/W(x)}, & \text{if } x \in \Omega(t) \\ F_0(x), & \text{otherwise} \end{cases}, \quad (6)$$

where $F_0(x)$ is the initial fuel supply and $W(x)$ is the time constant of the fuel. The heat flux from the fire to the atmosphere is given by the amount of fuel burned

$$H = -A(x) \frac{d}{dt} F(x, t) = \begin{cases} F_0(x) \frac{e^{-(t-t_i(x))/W(x)}}{W(x)}, & \text{if } x \in \Omega(t), \\ 0, & \text{otherwise.} \end{cases} \quad (7)$$

The coefficients c_0 , R_0 , S_{\max} , a , b , d , W , and A characterize the fuel and they are determined from laboratory experiments.

This model was developed in [10], where a tracer scheme was used to advance the fireline. Tracer schemes do well when advecting the shape of the fire in a wind, but they require complicated code for numerous special cases when the topology of the fireline changes, such as when fire fronts merge. Also, tracer schemes are not well suited for data assimilation. Changing the location of a fireline represented by tracers would require a special, complicated code, and the state of the model cannot be adjusted by making corrections to gridded arrays, as is usual in data assimilation methods.

Possible implementation of the propagation of the fireline is the level set method. The level set method evolves a function $\psi = \psi(x, t)$, called the *level set function*, such that the burning area is $\Omega(t) = \{x : \psi(x, t) < 0\}$ and the fireline is the level set

$$\Gamma(t) = \{x : \psi(x, t) = 0\}.$$

The level set function satisfies the differential equation

$$\frac{\partial \psi}{\partial t} + S(x) \|\nabla \psi\| = 0, \quad (8)$$

which is solved numerically. The state of the model is the level set function ψ and the ignition time t_i , defined by their values on grid nodes, so they can be modified by data assimilation methods in the usual manner. For further details, see “Level set methods.” A typical mesh step size for a fireline propagation code is 10m – 50m.

C. Coupling fire and weather models

The fire model can be either a reaction-diffusion formulation like (1) – (4) or a semi-empirical formulation like (5) – (8), where the surface fire rate of spread is imposed as a function of wind and terrain slope. In either case, the fire model takes as input the horizontal wind velocity \vec{v} and it outputs the heat flux H , given by (2) or (7). The wind velocity should be the ambient wind that would exist when no fire is present. A small backing rate of spread must be specified, since fires are known to creep upwind on their upwind edge due to radiation.

In [10], the Clark-Hall atmospheric code [11] was used. This code can nest and refine meshes from synoptic scale (10^2 km) to fire scale (10 m) horizontally and also refine meshes vertically. The Weather Research and Forecasting code (WRF, [53]) is used in the current work, because it is a standard for weather forecasting and because of its amenability to data assimilation. The

WRF code supports distributed memory execution and import/export of state with metadata (such as variable name, units, and geographical coordinates) for data assimilation. A typical horizontal mesh size for WRF for weather modeling is about 1 km, based on the spatial scales needed for modeling clouds, although the numerical approximations of the dynamical equations support finer resolution. Meshes are refined only horizontally, which means that the finest atmospheric mesh, which interfaces with the fire, goes from the surface of the Earth to the top. The recommended time step is proportional to the finest atmospheric mesh step, and equals to 1s for the minimal mesh step of 1 km.

For the fire model (1) – (4), the state is the temperature T and the fuel supply F . The state of fire model (5) – (8) is the level function ψ and the ignition time t_i , which records the level function history. At the beginning of an atmospheric time step, the wind is interpolated from the atmospheric mesh to the nodes of the fire mesh. The fire model is then advanced using a number of internal time steps to the end of the atmospheric time step, upon which the total heat flux H generated over the atmospheric time step is inserted in the atmospheric model. The heat flux includes sensible heat flux (a transfer of heat between the surface and air due to the difference in temperature between them) and latent heat flux (the transfer of heat due to the phase change of water between liquid and gas) given by the fuel type and its moisture. A difficulty is that it is ineffective to apply a heat flux directly as a boundary condition to an atmospheric model on the derivatives of the corresponding physical field (air temperature or water vapor contents) because atmospheric models use numerical methods explicit in time. Imposing a flux boundary condition with an explicit timestepping method directly would add all heat or vapor influx into a boundary layer one cell thick, requiring diffusion and convection to transport the heat further into the domain. Thus, the flux would result in a large non-physical change in temperature or vapor concentration in that boundary layer, and its effect would only get resolved over a number of time steps, progressing only one mesh cell away from the boundary in every time step. Implicit timestepping methods do not suffer from such ill effect, because the global problem solved in each time step forces all physical fields to be in balance at the end of the time step. Therefore, an empirical procedure is used, and the flux is inserted by modifying the temperature and water vapor concentration over a depth of many cells, with exponential decay away from the boundary. This decay mimics the distribution of temperature and water vapor fields arising from the vertical flux divergence. It is supported by infrared observations of the dynamics of crown fires in [16].

II. HIGH-PERFORMANCE IMPLEMENTATION OF THE ENKF

Now we describe the variant we have used as the base EnKF algorithm. Since the model states and the number of data points are very large, and the code needs to run much faster than real time, efficient massively parallel implementation is essential. This section is based on [40], where more details can be found. We start by recalling the Kalman filter formulas.

A. The Kalman formulas as Bayesian update for Gaussian distributions

Let \mathbf{x} denote the n -dimensional state vector of a model, and assume that it has Gaussian probability density function (pdf) $p(\mathbf{x})$ with mean μ and covariance Q . This probability distribution, called the *prior*, was evolved in time by running the model and now is to be updated to account for new data. Given state \mathbf{x} , the data \mathbf{d} is assumed to have Gaussian distribution

$p(\mathbf{d}|\mathbf{x})$, called *data likelihood*, with covariance R and mean $H\mathbf{x}$. The matrix H is called an *observation matrix*. The value $H\mathbf{x}$ is what the value of the data would be for the state \mathbf{x} in the absence of data errors, and the data covariance describes an estimate of the data errors; that is, the state should satisfy (in statistical sense) the *observation equation*

$$H\mathbf{x} = \mathbf{d}. \quad (9)$$

The pdf of the state and the data likelihood are combined to give the new probability density of the system state \mathbf{x} conditional on the value of the data \mathbf{d} (the *posterior*) by the Bayes theorem

$$p(\mathbf{x}|\mathbf{d}) = \frac{p(\mathbf{y}|\mathbf{d}) p(\mathbf{y})}{\int p(\mathbf{z}|\mathbf{d}) p(\mathbf{z}) d\mathbf{z}}.$$

The data \mathbf{d} is fixed once it is received, so denote the posterior state by $\hat{\mathbf{x}}$ instead of $\mathbf{x}|\mathbf{d}$ and the posterior pdf by $p(\hat{\mathbf{x}})$. The algebraic manipulations [2] show that the posterior pdf is also Gaussian with the posterior mean $\hat{\mu}$ and covariance \hat{Q} given by the Kalman update formulas

$$\hat{\mu} = \mu + K(\mathbf{d} - H\mu), \quad \hat{Q} = (I - KH)Q,$$

where

$$K = QH^T (HQH^T + R)^{-1}$$

is the so-called Kalman gain matrix.

B. The EnKF as a Monte Carlo approximation

Suppose $\mathbf{x}_1, \dots, \mathbf{x}_N$ is a random sample from the prior and the matrix X consists of $[\mathbf{x}_1, \dots, \mathbf{x}_N]$ as columns, $X = [\mathbf{x}_1, \dots, \mathbf{x}_N] = [\mathbf{x}_i]$. Replicate the data \mathbf{d} into an $m \times N$ matrix $D = [\mathbf{d}_1, \dots, \mathbf{d}_N] = [\mathbf{d}_i]$ so that each column \mathbf{d}_i consists of the data vector \mathbf{d} plus a random vector from the n -dimensional normal distribution with zero mean and covariance matrix R . Then the columns of

$$\hat{X} = X + K(D - HX) \quad (10)$$

form a random sample from the posterior distribution. The EnKF consists of the Bayesian step (10) with two approximations: 1. the mean and the covariance of the pdf of the prior are replaced by the sample mean and covariance computed from the ensemble; 2. even if the ensemble members are really not a random sample, because they are not independent – the EnKF ties them together in every Bayesian step. With these approximations, the posterior ensemble is

$$X^a = X + CH^T \underbrace{(HCH^T + R)^{-1}}_P (D - HX), \quad (11)$$

where

$$C = \frac{AA^T}{N-1}, \quad A = X - \frac{1}{N} (X\mathbf{e}_{N \times 1}) \mathbf{e}_{1 \times N}, \quad (12)$$

and \mathbf{e} denotes the matrix of all ones of the indicated size. From (12), it follows that $C = XM$ for some matrix M . Consequently, *the posterior ensemble consists of linear combinations of the prior ensemble*.

C. Efficient matrix implementation of EnKF formulas

Note that since R is a covariance matrix, it is always positive semidefinite, and typically positive definite. Then P^{-1} exists and the formula (11) can be implemented efficiently by the Choleski decomposition. The formulas (11) – (12) are same as in [7], except that [7] uses the sample covariance $DD^T/(N-1)$ and the inverse then needs to be replaced by a pseudoinverse, computed by the Singular Values Decomposition (SVD), which is more expensive. Also, instead of computing the inverse of a matrix and multiplying by it, it is much better (several times cheaper, more accurate, and standard practice) to compute the Choleski decomposition of the matrix and implement the multiplication by the inverse as solution of a linear system with many simultaneous right-hand sides [31]. Since the EnKF formulas are written as matrix algebra with dominant Level 3 (dense matrix-matrix) operations [31], they are suitable for efficient implementation using software packages such as LAPACK (on serial and shared memory computers) and ScaLAPACK [18] (on distributed memory computers).

For a large number m of data points, such as in the assimilation of gridded data or images, the Choleski decomposition of the matrix P becomes a bottleneck. A better way is possible when the data error covariance matrix R is diagonal (which is the case when the data errors are uncorrelated), or at least cheap to decompose (such as block diagonal or banded due to limited covariance distance). Using the Sherman-Morrison-Woodbury formula [33]

$$(R + UV^T)^{-1} = R^{-1} - R^{-1}U(I + V^T R^{-1}U)^{-1}V^T R^{-1}$$

with $U = \frac{1}{N-1}HA$ and $V = HA$ gives

$$\begin{aligned} P^{-1} &= \left(R + \frac{1}{N-1}HA(HA)^T \right)^{-1} \\ &= R^{-1} \left[I - \frac{1}{N-1}(HA) \left(I + (HA)^T R^{-1} \frac{1}{N-1}(HA) \right)^{-1} (HA)^T R^{-1} \right], \end{aligned} \quad (13)$$

which requires only the solutions of systems with the matrix R (assumed to be cheap) and of a system of size N with m right-hand sides. See [40] for operation counts.

If R is diagonal, it is also possible to assimilate the data points sequentially, since then the observations are independent, but level 3 operations (matrix-matrix, that is, many vectors at a time) are more efficient than repeated level 2 matrix-vector operations on one vector at a time.

Finally, it is inconvenient to construct and operate with the matrix H explicitly; instead, we wish to evaluate a function $h(x)$ of the form

$$h(\mathbf{x}) = H\mathbf{x} + \mathbf{f}, \quad (14)$$

where H and \mathbf{f} are fixed but unknown, and instead of (9), use the observation equation $h(\mathbf{x}) = \mathbf{d}'$, where $\mathbf{d} = \mathbf{d}' - \mathbf{f}$. The function h is called the *observation function* or, in the inverse problems context, the *forward operator*. The value of $h(\mathbf{x})$ is what the value of the data \mathbf{d}' would be for the state \mathbf{x} assuming the measurement is exact. It is easy to see that H occurs in (11), (12), and (13) only in the expressions HA and $HX - D$, which is obtained by random perturbations of the columns $H\mathbf{x}_i - \mathbf{d}$. But the columns of the matrix-matrix product HA and the residuals

$H\mathbf{x}_i - \mathbf{d}$ can be evaluated by calling h once on every ensemble member

$$\begin{aligned} [HA]_i &= H\mathbf{x}_i - H\frac{1}{N}\sum_{j=1}^N \mathbf{x}_j \\ &= h(\mathbf{x}_i) - \frac{1}{N}\sum_{j=1}^N h(\mathbf{x}_j), \end{aligned}$$

$$\begin{aligned} H\mathbf{x}_i - \mathbf{d} &= H\mathbf{x}_i - (\mathbf{d}' - \mathbf{f}) \\ &= h(\mathbf{x}_i) - \mathbf{d}'. \end{aligned}$$

This approach has been commonly used for a nonlinear observation function h , such as the position of a hurricane vortex [8]. Essentially, it approximates the observation function by the linear interpolation from its values at the ensemble members.

D. EnKF in a high-performance computing environment

We are using an ensemble management scheme similar to one in the software package DART [3]. The analysis cycles are run in a shell script loop. Each ensemble member state is maintained in a separate collection of files. The input and output of WRF is in the standard NETCDF file format. The NETCDF files also contain the metadata needed to evaluate the observation function, such as geographical coordinates of mesh nodes.

In each cycle, all ensemble members are advanced in time, each member by a separate run of the simulation code. The simulation code is a parallel application, which executes on a collection of processors, both for speed and distribution of the memory use. If enough processors are available, some or all ensemble members are advanced concurrently. After all ensemble members are advanced in time, the EnKF code is started on all available nodes. The EnKF code loads the state of the ensemble members from the files, reads data to be assimilated from data files, calls subroutines to evaluate the various observation functions, and performs the EnKF calculations using high-performance parallel linear algebra. The modified states of ensemble members are written to files and the cycle repeats.

Running the EnKF and the simulations as a single parallel application with data passed in memory only is also possible, and it has been done [41] for the standalone reaction-diffusion equation fire model. However, running the EnKF and the simulations separately affords more flexibility, does not force integration of the codes into a single executable, and allows for natural checkpointing and restart of the data assimilation scheme.

For efficiency, on computer clusters with local filesystems on nodes, the files with the state of a member should be kept in local files on the nodes used to advance that member. Some computer systems, such as IBM BlueGene, have a single high-performance file system, designed for massively parallel access, with multiple independent high-speed links from subsets of nodes. In that case, simulations running on separate groups of nodes can access their files on the common filesystem without interference with each other.

III. ASSIMILATION OF DATA INTO FIRE MODELS

Because wildfire data may be sparse in space and time and the model solution may be inaccurate by the time the data arrive, the model state and the reality as measured by the data may be far apart, yet the simulation must recover and continue. Thus, an important quality of data assimilation methods is their ability to make large corrections to the state without breaking the assimilation method or the model.

Statistical variability of correction and especially large corrections may result in nonphysical states, which tend to be preceded or accompanied by large spatial gradients. In order to ease this problem, a *regularized EnKF* was developed [34], which penalizes large changes of spatial gradients in the Bayesian update. In the data assimilation framework, the regularization can be implemented by adding an independent observation $\nabla u = \nabla \bar{u}$, with normal error distribution with zero mean. Here u is one of the fields in model state (such as the temperature), ∇ is the spatial gradient, computed by finite differences, and \bar{u} is mean of the prior ensemble. Smaller error covariance means stronger penalization of large changes in the gradient. Because the added observation is independent of other data in the Bayesian update, it is easily implemented by running the EnKF formulas for the second time.

The regularization technique has a stabilizing effect on the simulations in the ensemble (Fig. 3), but it does not improve much the ability of the EnKF to track the data. The posterior ensemble is made out of linear combinations of the prior ensemble, and if a reasonably close location and shape of the fire cannot be found between the linear combinations, the data assimilation is simply out of luck, and the ensemble cannot approach the data. From that point on, the ensemble evolves essentially without regard to the data at all. This process is called filter divergence.

One explanation of filter divergence in this fire problem is that the EnKF is based on the assumption that all probability distributions involved are at least approximately Gaussian. While the location of the fire may have an error distribution that is approximately Gaussian, this phenomenon is certainly not the case for the value of the state (such as the temperature) at a given point. Instead, the probability distribution of the state at a given point near the fireline is concentrated around the burning and the not burning states. There is clearly a need to adjust the simulation state by a position rather than an additive correction. We use techniques from image processing for this purpose. Moving and stretching one given image to become another given image is known as registration [6]. Classical registration methods require a user to pick which points are to be transformed into which points, but fully automatic methods now exist. Once the two images are registered, one can easily create intermediate images, which is known as morphing. The intermediate images can be created in such a way that they can be used instead of linear combinations of states in EnKF. The resulting method, called *morphing EnKF* [5], provides both additive and position correction in a natural manner. Related methods in the literature include transformation of the space by a low order polynomial mapping [1] and solving a differential equation to find an alignment mapping as a preprocessing to an additive correction [37], [49].

Consider two functions u_0, u_1 , representing the same physical field, such as the temperature, or the level function, from two states of a wildfire model. The functions are represented by gridded arrays on the fire problem domain, and considered interpolated away from grid nodes. Let $x = (x_1, x_2)$ be coordinates of a point in the fire problem domain on the surface of the Earth. The registration problem is to find a mapping $T : x \mapsto T(x)$ such that the change of

variable $x \mapsto x + T(x)$ transforms u_0 into a function approximately equal to u_1 , $u_0(x + T(x)) \approx u_1(x)$. This process can be written in a compact form as

$$u_1 \approx u_0 \circ (I + T) \text{ on } D, \quad (15)$$

where \circ denotes the composition of mappings, and $I : x \mapsto x$ is the identity mapping. The mapping $I + T$ is called the *registration mapping*, and the mapping T is called *warping*. The reason for writing the registration mapping as $I + T$ is that the zero warping $T = 0$ is the neutral element of the operation of addition, and so linear combinations of warpings have a meaningful interpretation as blends of the warpings. This registration mapping is important in the development of the morphing EnKF.

To avoid unnecessarily large warping, T must be as close to zero and as smooth as possible

$$T \approx 0, \quad \nabla T \approx 0, \quad (16)$$

where ∇T denotes the matrix of the first derivatives (the Jacobian matrix) of T . In addition, we require that the registration mapping $I + T$ is one-to-one, so the inverse $(I + T)^{-1}$ exists. For a fully automatic method to construct such a mapping T , see “Image registration.” The mapping T is represented by its values on a *morphing grid*, which is generally coarser than the fire grid, and interpolated away from the grid points. Because models often do not take well kinks appearing in their physical fields, we choose tensor product cubic spline interpolation, so ∇T is continuous.

Once the registration mapping $I + T$ is found, one can construct intermediate functions u_λ between u_0 and u_1 . Perhaps the simplest way to do that would be by the change of variable

$$u_\lambda = u_0 \circ (I + \lambda T), \quad 0 \leq \lambda \leq 1.$$

This formula, however, only entails changes in position, and not change in value. As a result, it does not give a continuous transition between u_0 and u_1 as λ changes from 0 to 1, because, in general, the equality in (15) is only approximate, so $u_1 \neq u_0 \circ (I + \lambda T)$. We could add a correction for the change of value, growing linearly between u_0 and u_1 , to get a continuous transition between u_0 and u_1 by

$$u_\lambda = u_0 \circ (I + \lambda T) + \lambda (u_1 - u_0 \circ (I + T)), \quad 0 \leq \lambda \leq 1.$$

Unfortunately, the added correction in value is always in the same position, which is not desirable. When the difference in (15) is not negligibly small, the intermediate functions u_λ has a spurious feature in the fixed location where the difference is large. To achieve a transition that blends naturally the change in position and value, we use the morphing formula from [5]

$$u_\lambda = (u + \lambda r) \circ (I + \lambda T), \quad 0 \leq \lambda \leq 1, \quad (17)$$

where

$$r = u_1 \circ (I + T)^{-1} - u_0. \quad (18)$$

The original functions u_0 and u_1 are recovered by choosing in (17) $\lambda = 0$ and $\lambda = 1$. The formula (17) is more complicated and expensive because of the inverse $(I + T)^{-1}$. The evaluation of $y = (I + T)^{-1}x$ can be done by the inverse interpolation. Let y_i be the grid nodes, and define $x_i = (I + T)y_i$. Then an approximate value of y is obtained by interpolating the values of y_i on the nonuniform grid formed by the mapped nodes x_i .

The morphing EnKF works by transforming the member states into extended states $[r, T]$ consisting of additive and position components that encode the difference of the member from a base state u_0 . The EnKF formulas are run on the extended states $[r, T]$. Then the extended states are converted back by (17) and advanced in time. The base state u_0 can be created by taking the average of the extended states $[r, T]$ after the EnKF update, transforming back, and advancing in time. Alternatively, the base state can be chosen as one of the ensemble members, or, for short simulation times, the base state may be fixed as the initial state that the ensemble was created from.

The morphing EnKF has been demonstrated to be able to make a large correction in the state and track the data in an accurate and stable manner for the reaction-diffusion model (Fig. 5) as well as for the fireline propagation model (Fig. 6) alone and coupled with WRF (Fig. 7).

IV. CONCLUSION

We have described several wildland fire models and methods for assimilating data in those modes. The EnKF was implemented in a distributed-memory high-performance computing environment. Data assimilation methods were developed combining EnKF with Tikhonov regularization to avoid nonphysical states and with the ideas of registration and morphing from image processing to allow large position corrections. The data assimilation methods can track the data even in the presence of the large correction, and avoid divergence. The methods can assimilate gridded data, but the assimilation of station data and steering of data acquisition is left to future developments.

V. ACKNOWLEDGMENTS

This research was supported by NSF grants CNS-0325314, CNS-0324910, CNS-0719641, and DMS-0623983, and by NCAR Faculty Fellowship for the first author. Computer time on IBM BlueGene/L supercomputer was provided by NSF MRI Grants CNS-0421498, CNS-0420873, and CNS-0420985, NSF sponsorship of the National Center for Atmospheric Research (NCAR), the University of Colorado, and a grant from the IBM Shared University Research (SUR) program.

The authors would like to thank Craig Douglas, Deng Li, Wei Li, and Adam Zornes from the University of Kentucky for their contributions to the software infrastructure that some of the codes used here were built on, John Michalakes from NCAR for his assistance with WRF, and Ned Patton from NCAR for providing his prototype code for interfacing an earlier fireline propagation model with WRF.

REFERENCES

- [1] G. D. ALEXANDER, J. A. WEINMAN, AND J. L. SCHOLS, *The use of digital warping of microwave integrated water vapor imagery to improve forecasts of marine extratropical cyclones*, Monthly Weather Review, 126 (1998), pp. 1469–1496.
- [2] B. D. O. ANDERSON AND J. B. MOORE, *Optimal filtering*, Prentice-Hall, Englewood Cliffs, N.J., 1979.
- [3] J. L. ANDERSON, *Data Assimilation Research Testbed – DART*. <http://www.image.ucar.edu/DAReS/DART/>, 2007.
- [4] M. I. ASENSIO AND L. FERRAGUT, *On a wildland fire model with radiation*, Int. J. Numer. Meth. Engrg., 54 (2002), pp. 137–157.
- [5] J. D. BEEZLEY AND J. MANDEL, *Morphing ensemble Kalman filters*, Tellus, 60A (2008), pp. 131–140.
- [6] L. G. BROWN, *A survey of image registration techniques*, ACM Computing Surveys, 24 (1992), pp. 325–376.
- [7] G. BURGERS, P. J. VAN LEEUWEN, AND G. EVENSEN, *Analysis scheme in the ensemble Kalman filter*, Monthly Weather Review, 126 (1998), pp. 1719–1724.
- [8] Y. CHEN AND C. SNYDER, *Assimilating vortex position with an ensemble Kalman filter*, Monthly Weather Review, 135 (2007), pp. 1828–1845.
- [9] N. P. CHENEY, J. S. GOULD, AND W. R. CATCHPOLE, *The influence of fuel, weather, and fire shape variables on fire-spread in grasslands*, International Journal of Wildland Fire, 3 (1993), pp. 31–44.
- [10] T. L. CLARK, J. COEN, AND D. LATHAM, *Description of a coupled atmosphere-fire model*, Intl. J. Wildland Fire, 13 (2004), pp. 49–64.
- [11] T. L. CLARK AND W. D. HALL, *On the design of smooth, conservative vertical grids for interactive grid nesting with stretching*, J. Appl. Meteor., 35 (1996), pp. 1040–1046.
- [12] T. L. CLARK, M. A. JENKINS, J. COEN, AND D. PACKHAM, *A coupled atmospheric-fire model: Convective feedback on fire line dynamics*, J. Appl. Meteor., 35 (1996), pp. 875–901.
- [13] T. L. CLARK, M. A. JENKINS, J. COEN, AND D. PACKHAM, *A coupled atmospheric-fire model: Convective Froude number and dynamic fingering*, Intl. J. of Wildland Fire, 6 (1996), pp. 177–190.
- [14] J. L. COEN, *Simulation of the Big Elk Fire using coupled atmosphere-fire modeling*, International J. of Wildland Fire, 14 (2005), pp. 49–59.
- [15] J. L. COEN, T. L. CLARK, AND D. LATHAM, *Coupled atmosphere-fire model simulations in various fuel types in complex terrain*, in 4th. Symp. Fire and Forest Meteor. Amer. Meteor. Soc., Reno, Nov. 13–15, 2001, pp. 39–42.
- [16] J. L. COEN, S. MAHALINGAM, AND J. W. DAILY, *Infrared imagery of crown-fire dynamics during FROSTFIRE*, J. Appl. Meteor., 43 (2004), pp. 1241–1259.
- [17] F. DAREMA, *Dynamic data driven applications systems: A new paradigm for application simulations and measurements*, in Computational Science-ICCS 2004: 4th International Conference, M. Bubak, G. D. van Albada, P. M. A. Sloot, and J. J. Dongarra, eds., vol. 3038 of Lecture Notes in Computer Science, Springer, 2004, pp. 662–669.
- [18] J. DONGARRA AND L. S. BLACKFORD, *Scalapack tutorial*, in Applied Parallel Computing: Industrial Computing and Optimization (Proceedings of the Third Int. Workshop PARA’96, Lyngby, Denmark), J. Wasniewski, J. Dongarra, K. Madsen, and D. Olsen, eds., Springer Verlag, Heidelberg, 1996, pp. 204–215. <http://www.netlib.org/utk/papers/scalapack-tutorial.ps>.
- [19] A. DOUCET, N. DE FREITAS, AND N. GORDON, eds., *Sequential Monte Carlo in Practice*, Springer, 2001.
- [20] J.-L. DUPUY AND M. LARINI, *Fire spread through a porous forest fuel bed: A radiative and convective model including fire-induced flow effects*, International J. of Wildland Fire, 9 (1999), pp. 155–172.
- [21] H. W. EMMONS, *Fire in the forest*, Fire Research Abstracts and Reviews, 5 (1963), p. 163.
- [22] D. ENRIGHT, F. LOSASSO, AND R. FEDKIW, *A fast and accurate semi-Lagrangian particle level set method*, Comput. & Structures, 83 (2005), pp. 479–490.
- [23] G. EVENSEN, *Data assimilation: The ensemble Kalman filter*, Springer, Berlin, 2007.
- [24] F. E. FENDELL AND M. F. WOLFF, *Wind-aided fire spread*, in Forest fires, behavior and ecological effects, E. A. Johnson and K. Miyanishi, eds., Academic Press, San Diego, CA, 2001, pp. 171–223.
- [25] M. A. FINNEY, *FARSITE: Fire area simulator-model development and evaluation*. Res. Pap. RMRS-RP-4, Ogden, UT: U.S. Department of Agriculture, Forest Service, Rocky Mountain Research Station. 47 p., <http://www.farsite.org>, 1998.
- [26] W. L. FONS, *Analysis of fire spread in light fuels*, Journal of Agricultural Research, 72 (1946), pp. 93–121.
- [27] FORESTRY CANADA FIRE DANGER GROUP, *Development and structure of the canadian forest fire behavior prediction system*. Forestry Canada, Science and Sustainable Development Directorate, Ottawa, ON, Information Report ST-X-3, 1992.
- [28] D. A. FRANK-KAMENETSKII, *Diffusion and heat exchange in chemical kinetics*, Princeton University Press, 1955.
- [29] P. FROLKOVIĆ AND K. MIKULA, *Flux-based level set method: a finite volume method for evolving interfaces*, Appl. Numer. Math., 57 (2007), pp. 436–454.
- [30] P. GAO AND T. W. SEDERBERG, *A work minimization approach to image morphing*, The Visual Computer, 14 (1998), pp. 390–400.
- [31] G. H. GOLUB AND C. F. V. LOAN, *Matrix Computations*, Johns Hopkins Univ. Press, 1989. Second Edition.
- [32] P. GRINDROD, *The theory and applications of reaction-diffusion equations: Patterns and waves*, Oxford Applied Mathematics and Computing Science Series, The Clarendon Press Oxford University Press, New York, second ed., 1996.
- [33] W. W. HAGER, *Updating the inverse of a matrix*, SIAM Rev., 31 (1989), pp. 221–239.

- [34] C. J. JOHNS AND J. MANDEL, *A two-stage ensemble Kalman filter for smooth data assimilation*. Environmental and Ecological Statistics, in print. Published online, DOI 10.1007/s10651-007-0033-0, 2007. Conference on New Developments of Statistical Analysis in Wildlife, Fisheries, and Ecological Research, Oct 13-16, 2004, Columbia, MI.
- [35] E. KALNAY, *Atmospheric Modeling, Data Assimilation and Predictability*, Cambridge University Press, 2003.
- [36] R. KREMENS, J. FAULRING, AND C. C. HARDY, *Measurement of the time-temperature and emissivity history of the burn scar for remote sensing applications*. Paper J1G.5, Proceedings of the 2nd Fire Ecology Congress, Orlando FL, American Meteorological Society, 2003.
- [37] W. G. LAWSON AND J. A. HANSEN, *Alignment error models and ensemble-based data assimilation*, Monthly Weather Review, 133 (2005), pp. 1687–1709.
- [38] R. LINN, J. REISNER, J. J. COLMAN, AND J. WINTERKAMP, *Studying wildfire behavior using FIRETEC*, Int. J. of Wildland Fire, 11 (2002), pp. 233–246.
- [39] V. MALLET, D. E. KEYES, AND F. E. FENDELL, *Modeling wildland fire propagation with level set methods*. arXiv:0710.2694, 2007.
- [40] J. MANDEL, *Efficient implementation of the ensemble Kalman filter*. CCM Report 231, University of Colorado Denver, 2006.
- [41] J. MANDEL, J. D. BEEZLEY, L. S. BENNETHUM, J. L. C. SOHAM CHAKRABORTY, C. C. DOUGLAS, J. HATCHER, M. KIM, AND A. VODACEK, *A dynamic data driven wildland fire model*, in Computational Science-ICCS 2007: 7th International Conference, Y. Shi, G. D. van Albada, P. M. A. Sloot, and J. J. Dongarra, eds., vol. 4487 of Lecture Notes in Computer Science, Springer, 2007, pp. 1042–1049.
- [42] J. MANDEL, L. S. BENNETHUM, J. D. BEEZLEY, J. L. COEN, C. C. DOUGLAS, L. P. FRANCA, M. KIM, AND A. VODACEK, *A wildfire model with data assimilation*. CCM Report 233, <http://www.math.cudenver.edu/ccm/reports>, 2006.
- [43] E. MARCHANDISE, J.-F. REMACLE, AND N. CHEVAUGEON, *A quadrature-free discontinuous Galerkin method for the level set equation*, J. Comput. Phys., 212 (2006), pp. 338–357.
- [44] W. MELL, M. A. JENKINS, J. GOULD, AND P. CHENEY, *A physics-based approach to modelling grassland fires*, Intl. J. Wildland Fire, 16 (2007), pp. 1–22.
- [45] I. R. NOBLE, G. A. V. BARY, AND A. M. GILL, *Mcarthurs fire danger meters expressed as equations*, Australian Journal of Ecology, 5 (1980), pp. 201–203.
- [46] S. OSHER AND R. FEDKIW, *Level set methods and dynamic implicit surfaces*, vol. 153 of Applied Mathematical Sciences, Springer-Verlag, New York, 2003.
- [47] S. OSHER AND J. A. SETHIAN, *Fronts propagating with curvature-dependent speed: algorithms based on Hamilton-Jacobi formulations*, J. Comput. Phys., 79 (1988), pp. 12–49.
- [48] B. PORTERIE, D. MORYAN, J. LORAUD, AND M. LARINI, *A multiphase model for predicting line fire propagation*, in Forest Fire Research: Proceedings 3rd International Conference on Forest Fire Research and 14th Conference on Fire and Forest Meteorology, Louso, Coimbra, Portugal, 16–18 November, 1998, D. X. Viegas, ed., vol. 1, Associação para o Desenvolvimento da Aerodinamica Industrial, 1998, pp. 343–360.
- [49] S. RAVELA, K. A. EMANUEL, AND D. McLAUGHLIN, *Data assimilation by field alignment*, Physica D, 230 (2007), pp. 127–145.
- [50] G. D. RICHARDS, *Numerical simulation of forest fires*, Internat. J. Numer. Methods Engrg., 25 (1988), pp. 625–633. Numerical methods in thermal problems (Montreal, PQ, 1987).
- [51] R. C. ROTHERMEL, *A mathematical model for predicting fire spread in wildland fires*. USDA Forest Service Research Paper INT-115, January 1972.
- [52] J. A. SETHIAN, *Level set methods and fast marching methods*, vol. 3 of Cambridge Monographs on Applied and Computational Mathematics, Cambridge University Press, Cambridge, second ed., 1999.
- [53] WRF WORKING GROUP, *Weather Research Forecasting (WRF) Model*. <http://www.wrf-model.org>, 2005.

VI. AUTHOR INFORMATION

Jan Mandel is Professor of Mathematics and Adjunct Professor of Computer Science at the University of Colorado Denver, Denver, CO, and visiting scientist at the National Center for Atmospheric Research, Boulder, CO, email `Jan.Mandel@cudenver.edu`. He received a PhD in Numerical Mathematics from the Charles University, Prague, Czech Republic, in 1983. He has developed domain decomposition and multilevel iterative solvers for large problems of equations from finite elements. He is interested in high-performance computing, wildfire modeling, data assimilation, and foundations in probability theory.

Jonathan D. Beezley is a PhD student of Applied Mathematics at the University of Colorado Denver and visiting graduate student at the National Center for Atmospheric Research, Boulder, CO. He is interested in ensemble filters, parallel software, and image registration.

Janice L. Coen is a project scientist at the National Center for Atmospheric Research, Boulder, CO. She received a PhD in Geophysical Sciences from the University of Chicago in 1992. Her interests are in mesoscale meteorology and wildland fire behavior. She has developed components of a coupled atmosphere-fire model and led the implementation of an operational weather forecasting system for the United Arab Emirates.

Minjeong Kim is a PhD student of Applied Mathematics at the University of Colorado Denver. She is interested in numerical schemes for level set methods and in wildfire modeling by partial differential equations.

VII. SIDEBAR - WILDLAND FIRE MODELING

The purpose of wildland fire modeling is to understand and ultimately predict fire behavior in order to increase safety of firefighters and the public, to reduce risk and minimize damage, and to protect ecosystems, watersheds, and air quality.

A. What is fire modeling?

The process of fire modeling aims to reproduce and anticipate properties of fire behavior and fire effects. Fire behavior includes the rate of spread of the flaming front (the interface between burning and unburned fuel), the heat release rate which is related to the burning intensity, as well as specific phenomena such as the bending forward of the fire front, transition from surface to crown fires, and extreme fire activity such as firewhirls. Fire effects which include ecological and hydrological effects on the landscape, such as the percentage of forest fuel consumed in prescribed fires, mortality suffered by trees, or the quantity of smoke produced for health impacts.

Three environmental factors affect wildland fire behavior: weather, fuel characteristics, and topography. Fuel factors include the type, moisture, size, shape, amount, and arrangement. Topography factors include the orientation toward the sun, the slope, and features such as narrow canyons and barriers such as creeks, roads, and unburnable fuel. Of the three environmental factors, weather (including factors such as wind, temperature, relative humidity, and precipitation) is the most rapidly changing. Weather phenomena that bring changes such as cold fronts, foehn winds, thunderstorm downdrafts, sea and land breezes, and diurnal slope winds can be particularly dangerous, as they can suddenly change the fire's direction and behavior. Weather also influences wildfires through the other factors of fuel and topography, by controlling the fuel moisture through precipitation, RH, and winds, and by complicating the fire-accelerating effect of slopes with topographically-induced accelerations. These factors are not independent - weather and terrain combine to produce topographic effects such as downslope windstorms (called Santa Annas, foehn winds, East winds, depending on the geographic location), the weather influences fuel moisture as dry winds or precipitation increases or decreases evaporation of moisture and therefore the fuel moisture, and fuel properties may vary with topography as plant density varies with elevation or aspect with respect to the sun. And, though weather can influence wildfire behavior through many pathways, it has long been recognized that fires 'create their own weather'. That is, the heat and moisture created by the fire feed back into the atmosphere, creating intense winds that drive the fire's behavior, sometimes overwhelming the effect of ambient winds.

B. How do people do fire modeling

Wildland fire models span a vast range of complexity, from simple cause and effect principles to the most physically complex presenting a difficult supercomputing challenge that cannot hope to be solved faster than real time. Conceptual models from experience and intuition from past fires can be used to anticipate the future. Many semi-empirical fire spread equations as in [51], [27], and [45] and [9] for Australasian fuel complexes have been developed for quick estimation of fundamental parameters of interest such as fire spread rate, flame length, and fireline intensity of surface fires at a point for specific fuel complexes, assuming a representative point-location

wind and terrain slope. Based upon the work in [26] and [21] the quasi-steady equilibrium spread rate calculated for a surface fire on flat ground in no-wind conditions was calibrated using data of piles of sticks burned in a flame chamber/wind tunnel to represent other wind and slope conditions for the fuel complexes tested. A simplified physically-based two-dimensional fire spread model based upon conservation laws that use radiation as the dominant heat transfer mechanism and convection, which represents the effect of wind and slope was developed in [4]. Two-dimensional fire growth models such as FARSITE [25] and Prometheus, the Canadian wildland fire growth model designed to work in Canadian fuel complexes, have been developed that apply such semi-empirical relationships and others regarding ground-to-crown transitions to calculate fire spread and other parameters along the surface. Certain assumptions must be made in models such as FARSITE and Prometheus to shape the fire growth for example, Prometheus and FARSITE use the Huygens principle of wave propagation. A set of equations that can be used to propagate (shape and direction) a fire front using an elliptical shape was developed in [50]. Although more sophisticated applications have used a three-dimensional numerical weather prediction system to provide inputs such as wind velocity to one of the fire growth models listed above, the input was passive and the feedback of the fire upon the atmospheric wind and humidity are not accounted for.

More complex physical models join computational fluid dynamics models with a wildland fire component and allow the fire to feed back upon the atmosphere. These include NCAR's Coupled Atmosphere-Wildland Fire-Environment (CAWFE) model developed in [14], Los Alamos National Laboratory's FIRETEC developed in [38], and the WUI (Wildland Urban Interface) Fire Dynamics Simulator (WFDS) [44] and, to some degree, the two-dimensional model PIF97 [20], [48]. These tools have different emphases and have been applied to better understand the fundamental aspects of fire behavior, such as fuel inhomogeneities on fire behavior [38], feedbacks between the fire and the atmospheric environment as the basis for the universal fire shape [15], [10], and are beginning to be applied to wildland urban interface house-to-house fire spread at the community-scale. The cost of added physical complexity is a corresponding increase in computational cost, so much so that a full three-dimensional explicit treatment of combustion in wildland fuels (so-called Direct Numerical Simulation (DNS)) at scales relevant for atmospheric modeling does not exist, is beyond current supercomputers, and does not currently make sense to do because of the limited skill of weather models at spatial resolution under 1 km. So, even these more complex models parameterize the fire in some way, for example, [13], [12] use [51] to calculate local fire spread rates using fire-modified local winds. And, although FIRETEC and WFDS carry prognostic conservation equations for the reacting fuel and oxygen concentrations, the computational grid cannot be fine enough to resolve the reaction rate-limiting mixing of fuel and oxygen, so approximations must be made concerning the subgrid-scale temperature distribution or the combustion reaction rates themselves. They also are too small-scale to interact with a weather model, so the fluid motions use a computational fluid dynamics model confined in a box much smaller than the typical wildfire. The limitations on fire modeling are not entirely computational. At this level, the models encounter limits in knowledge about the composition of pyrolysis products and reaction pathways, in addition to gaps in basic understanding about some aspects of fire behavior such as fire spread in live fuels and surface-to-crown fire transition.

Thus, while more complex models have value in studying fire behavior and testing fire spread in a range of scenarios, from the application point of view, FARSITE and Palm-based applications

of BEHAVE have shown great utility as practical in-the-field tools because of their ability to provide estimates of fire behavior in real time. While the coupled fire-atmosphere models have the ability to incorporate the ability of the fire to affect its own local weather, and model many aspects of the explosive, unsteady nature of fires that cannot be incorporated in current tools, it remains a challenge to apply these more complex models in a faster-than-real-time operational environment. Also, although they have reached a certain degree of realism when simulating specific natural fires, they must yet address issues such as identifying what specific, relevant operational information they could provide beyond current tools, how the simulation time could fit the operational time frame for decisions (therefore, the simulation must run substantially faster than real time), what temporal and spatial resolution must be used by the model, and how they estimate the inherent uncertainty in numerical weather prediction in their forecast. These operational constraints must be used to steer model development.

VIII. SIDEBAR - LEVEL SET METHODS

A. Curve evolution by the level set method

Consider a curve $\Gamma = \Gamma(t)$ in \mathbb{R}^2 evolving with the speed $S(x, t)$ in the normal direction. The level set method represents the curve as the level set

$$\Gamma = \{x : \psi(x, t) = 0\}$$

of a function ψ , called a level set function, and converts the evolution of the curve into a differential equation for the level set function, which is then solved numerically. In applications, the curve Γ is closed, and we choose that the inside of the curve is given by $\psi < 0$. Because $\psi = 0$ on Γ , the component of $\nabla\psi$ in the tangent direction is zero, and so $\nabla\psi$ has the normal direction to Γ . Thus, we can also use the level set function ψ to compute the normal to the curve Γ by

$$\vec{n} = \frac{\nabla\psi}{\|\nabla\psi\|},$$

where $\|\cdot\|$ is the Euclidean norm.

To derive an equation to evolve the level set function, consider a point $x = x(t) \in \Gamma(t)$. Then $\psi(x(t), t) = 0$, and from the chain rule

$$\begin{aligned} 0 &= \frac{d}{dt}\psi(x, t) \\ &= \frac{\partial\psi}{\partial t} + \underbrace{\nabla\psi}_{\|\nabla\psi\|\vec{n}} \cdot \frac{\partial x}{\partial t} \\ &= \frac{\partial\psi}{\partial t} + \|\nabla\psi\| \underbrace{\vec{n} \cdot \frac{\partial x}{\partial t}}_{S(x)}. \end{aligned}$$

Thus, the level set function is governed by the partial differential equation, called the level set equation [47] [52, Ch. 1]

$$\frac{\partial\psi}{\partial t} + S(x) \|\nabla\psi\| = 0.$$

Note that the level set equation requires propagation speed $S(x)$ to be defined at all points x , not just on the curve Γ .

When the initial curve Γ is a circle with center x_0 and radius s , the initial level set function can be chosen as

$$\psi(x) = \|x - x_0\| - s.$$

This initial is an example of a level set function as the signed distance function

$$\psi(x) = \pm \text{dist}(x, \Gamma),$$

with $-$ inside and $+$ outside of Γ . The signed distance function is characterized by $\|\nabla\psi\| = 1$. Ideally, ψ should be equal or close to the signed distance function for numerical stability, but this property is in general not preserved when advancing the level set equation in time.

B. Application to fireline propagation

In our computations, we have used the spread rate S defined by the Rothermel formula (5) at every point, not only the fireline. Thus, the fuel data and wind over the whole domain were used. The level set equation was discretized on a rectangular grid rectangular mesh with spacing $(\Delta x_1, \Delta x_2)$ and approximated by an explicit method with timestep Δt

$$\psi_{t+\Delta t} = \psi_t - \Delta t S(x, t) \|\psi_{x_1}, \psi_{x_2}\|,$$

where $[\psi_{x_1}, \psi_{x_2}]$ is a numerical approximation of the gradient of ψ . The Godunov method [46, p. 58] was used

$$\psi_{x_1} = \begin{cases} \psi_{x_1}^-, & \text{if } \psi_{x_1}^- \geq 0 \text{ and } \psi_{x_1}^- + \psi_{x_1}^+ \geq 0, \\ \psi_{x_1}^+, & \text{if } \psi_{x_1}^+ \leq 0 \text{ and } \psi_{x_1}^- + \psi_{x_1}^+ < 0, \\ 0, & \text{otherwise,} \end{cases}$$

where $\psi_{x_1}^-$ and $\psi_{x_1}^+$ are the left and the right one-sided numerical derivatives

$$\psi_{x_1}^-(x_1, x_2) = \frac{\psi(x_1 - \Delta x_1, x_2)}{\Delta x_1}, \quad \psi_{x_1}^+(x_1, x_2) = \frac{\psi(x_1 + \Delta x_1, x_2)}{\Delta x_1},$$

and similarly for $\psi_{x_2}^-$ and $\psi_{x_2}^+$. The use of a numerically stable scheme that includes upwinding, such as the Godunov scheme above, is required. When the gradient is approximated by standard central differences, the numerical method fails quickly. Since in the wildland fire application always $S \geq 0$, the level set function does not increase with time and the burnt area can only grow (Fig. S1).

The ignition time t_i in the strip that the fire has moved over in one timestep is computed by linear interpolation from the level function. Suppose that the point x is not burning at the time t but it is burning at the time $t + \Delta t$, that is, $\psi(x, t) > 0$ and $\psi(x, t + \Delta t) < 0$. The ignition time $t_i(x)$ at the point x satisfies $\psi(x, t_i) = 0$. Approximating ψ linearly in t , we have

$$\frac{\psi(x, t)}{t_i(x) - t} \approx -\frac{\psi(x, t + \Delta t)}{t_i - (t + \Delta t)},$$

which gives

$$t_i(x) \approx t + \frac{\psi(x, t) \Delta t}{\psi(x, t) - \psi(x, t + \Delta t)}.$$

The fuel burnt and thus the heat generated are then computed from the postulated exponential fuel decay (6).

For circular ignition with assumed spread rate R_0 , the ignition time can be initialized to

$$t_i(x) = t_0 + R_0 (\|x - x_0\| - s), \quad \|x - x_0\| \leq s,$$

which gives the time of ignition t_0 at the boundary of the circle and $t_0 - R_0 s$ at the center.

C. Related work

In [39], the narrow band level set method with velocity extension from the nearest point on the fireline was used to implement the fireline propagation model from [24]. The model postulates different spread rates at the head and the flanks of a fire and it does not consider the fuel balance or a coupling with the atmosphere.

One problem with level set methods is that they do not guarantee the *a-priori* conservation of the shape or volume of the level set even in a uniform constant velocity field. Because of the numerical dispersion inherent in upwinding schemes, the shape of level set function flattens up and the level set may either grow or decrease and eventually vanish. Also, details of the level set get smeared. Several sophisticated approaches have been developed to improve the conservation of the level set, such as the hybrid particle level set method [22], quadrature-free discontinuous Galerkin method [43], and flux based level set method [29].

IX. SIDEBAR - IMAGE REGISTRATION

Moving and stretching one given image to become another given image is known in image processing as registration [6]. The procedure outlined here can do that fully automatically, without a human intervention.

Given two function u and v on a domain D , the registration problem can be formulated as

$$v \approx u \circ (I + T) \text{ on } D.$$

At the same time, we wish that T and ∇T are not unnecessarily large. These requirements naturally leads to a construction of the mapping T by optimization

$$J(T) = \|v - u \circ (I + T)\| + C_1 \|T\| + C_2 \|\nabla T\| \rightarrow \min_T,$$

where $\|\cdot\|$ are suitable norms. We choose the $L^1(D)$ norms, $\|v\| = \int_D |v| dx$, evaluated by simple numerical integration. To define $\|T\|$ and $\|\nabla T\|$, we add the norms of the entries of the vector function T and the matrix function ∇T .

The optimization formulation tries to balance the conflicting objectives of good approximation by the registered image, and as small and smooth warping as possible. The objective function $J(T)$ is in general not a convex function of T , and there can be many local minima. For example, a local minimum may occur when some small part of u and v matches, while the overall match is still not very good.

To solve the optimization problem for the mapping T , we have used the algorithm from [30] with some modifications. The method proceeds by building the mapping T on a nested hierarchy of meshes, starting with a very coarse mesh that divides the domain D into just four rectangular cells. The mapping T is interpreted as the movement of grid nodes, and the nodes are moved one at a time to minimize a coarse version of $J(T)$. For each node, a mesh of a number of possible locations is constructed, all locations on the mesh are tested, then the location with the smallest value of $J(T)$ is selected and further improved by a standard descent method. In the coarse version of $J(T)$, the mapping T is interpolated from the nodes of the current grid, and the functions u and v are smoothed by a convolution to smear fine features and allow a more global match. The resulting mapping is then interpolated to a mesh that is twice finer, and the process continues. The final mesh on which T is computed is always coarser than the mesh on which the functions u and v are specified, because the same mesh would result in a T that is too oscillatory. See [5] for further details.

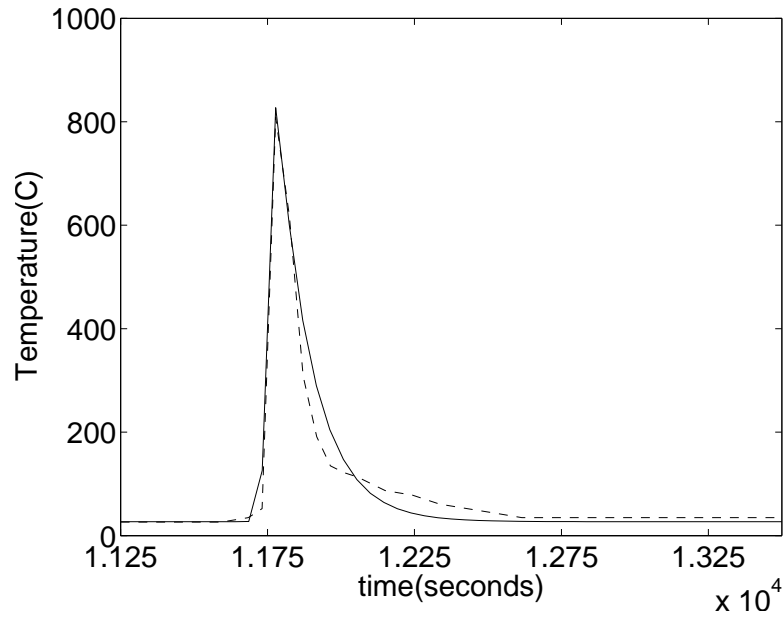


Fig. 1. Measured time-temperature profile (dash line) in a grass wildland fire at a fixed sensor location, digitized from [36], and computed profile (solid line) from a simulation by a numerical solution of the reaction-diffusion equations (1) – (4). Reproduced from [42].

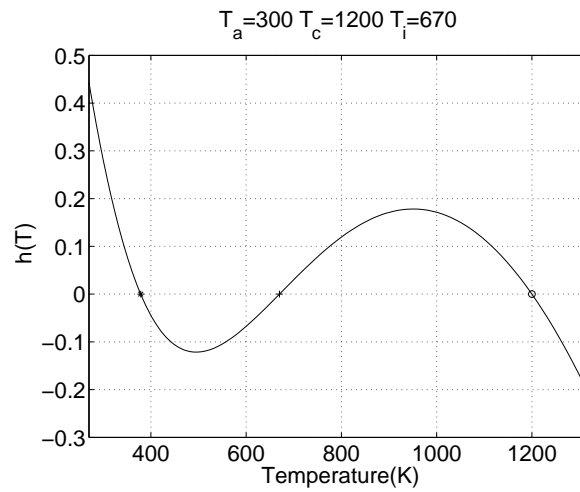


Fig. 2. An example of reaction heat balance function $h(T)$ from equation (1). The three zeros of the function are the ambient temperature T_a , the auto-ignition temperature T_i , and the high burning temperature T_c . Reproduced from [42].

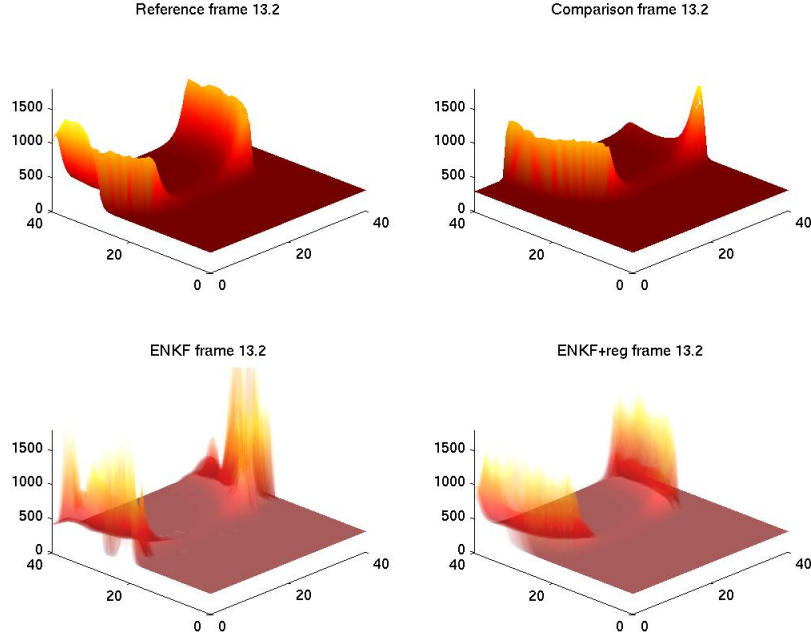


Fig. 3. Example of the effect of regularization by penalization of large change in gradients by the Bayesian update on propagation of fire. Circular spreading fire hits a fuel break in the middle of the domain. The horizontal axes are distance in m . The vertical axis is temperature in K . False color is generated from the temperature with shading for depth perception. The reference solution is the simulated data. In the comparison solution, the fire was started from intentionally incorrect location. The ENKF panel is the result of data assimilation after 13 cycles. The ENKF+reg panel is the ensemble after data assimilation after 13 cycles with regularization imposed in each cycle. The ensembles have 100 members and they are visualized as superposition of transparent images of their members. Both ensembles succeed in moving toward the data, but the regularized ensemble avoids the non-physical artefacts, such as extremely small and large temperatures.

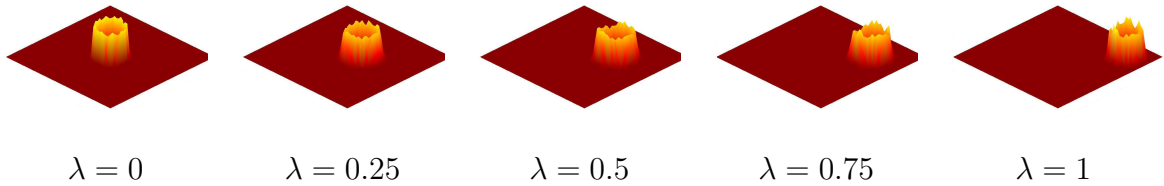


Fig. 4. Morphing of two solutions of a reaction-diffusion equation system (1) – (4) used in a wildfire simulation. The states with $\lambda = 0$ and $\lambda = 1$ are given. The intermediate states with $0 < \lambda < 1$ are created automatically by the morphing algorithm (17). The horizontal plane is the earth surface. The vertical axis and the color map are the temperature. The morphing algorithm combines the values as well as the positions. Reproduced from [5].

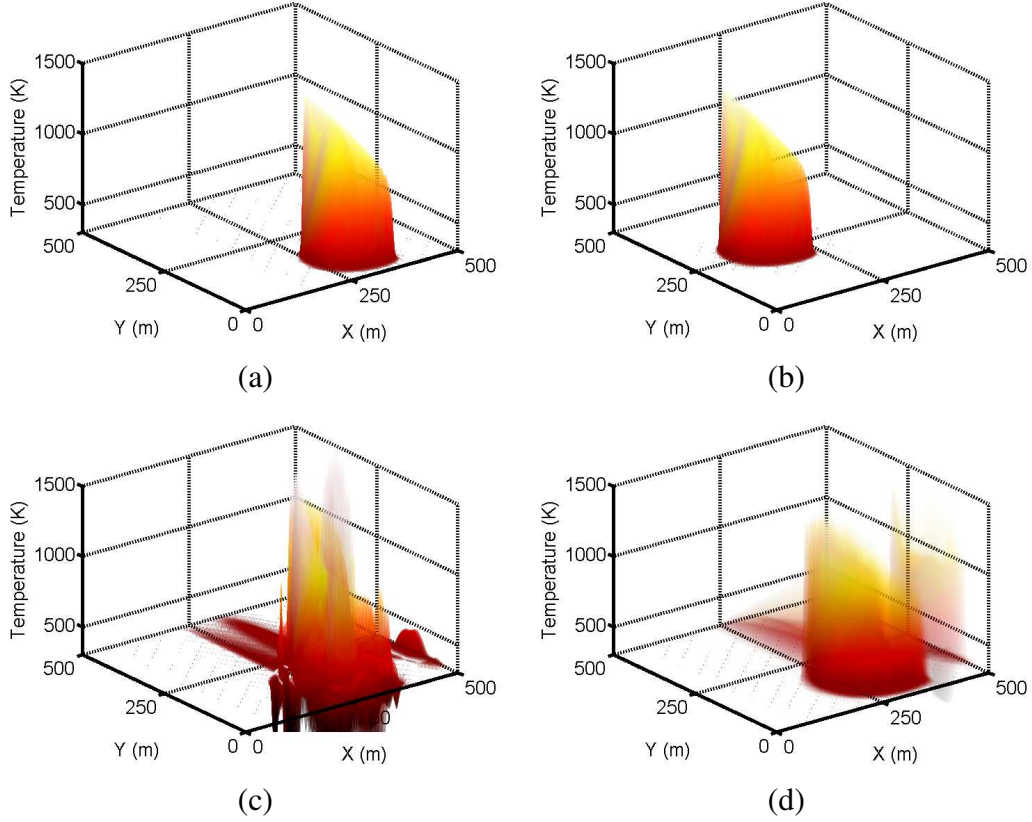


Fig. 5. The morphing EnKF applied to the reaction-diffusion model (1) – (4). False color is generated from the temperature with shading for depth perception. The reference solution (a) is the simulated data. The initial ensemble was created by a random perturbation of the comparison solution (b), where the fire was ignited at an intentionally incorrect location. The Standard ENKF panel (c) is the result of data assimilation of the temperature field after running the model for 500 seconds. The Morphing EnKF panel (d) is the ensemble with the image registration against the temperature field at the time of ignition, and applied to both the temperature and the fuel supply. The ensembles have 25 members each and they are visualized as superposition of transparent images of their members. The standard EnKF ensembles diverges from the data, while the Morphing EnKF ensemble tracks the data successfully.

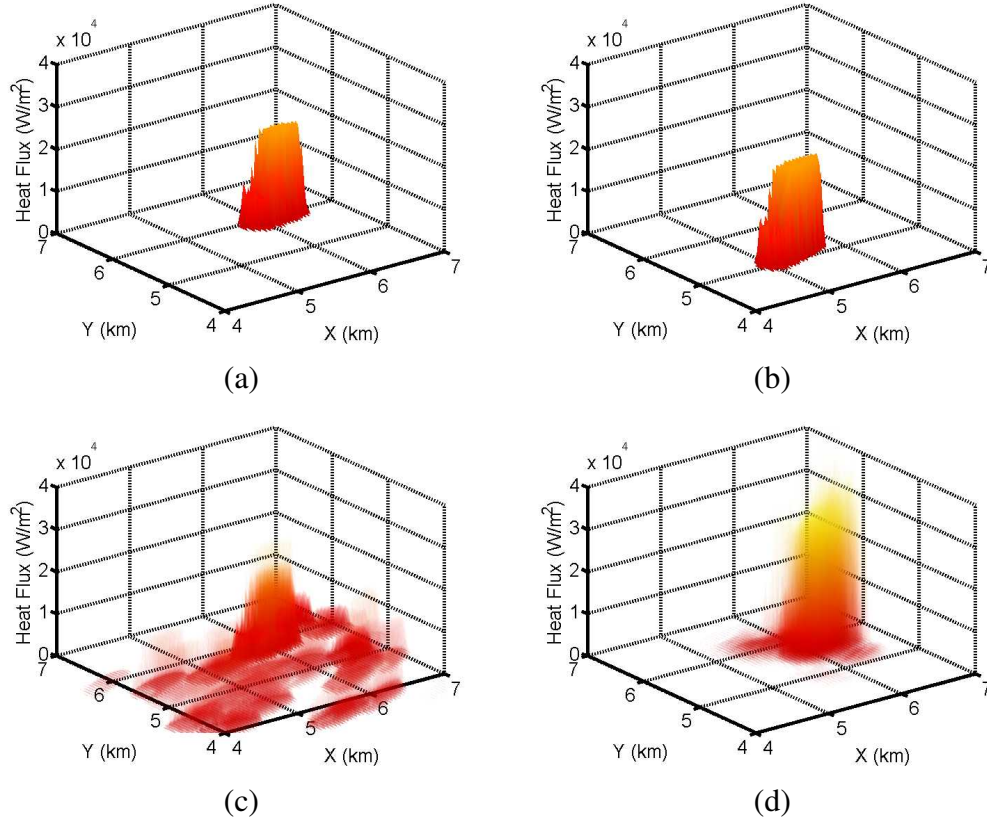


Fig. 6. The morphing EnKF applied to the fireline propagation model. False color is the output heat flux with shading for depth perception. The reference solution (a) is the simulated data. The initial ensemble was created by a random perturbation of the comparison solution (b), where the fire was ignited at an intentionally incorrect location. The Standard ENKF panel (c) is the result of data assimilation of the time from ignition after running the model for 1000 seconds. The Morphing EnKF panel (d) is the result with image registration determined from the time from ignition and applied to all of the model variables. The ensembles have 25 members each and they are visualized as superposition of transparent images of heat fluxes of their members. The standard EnKF ensembles diverges from the data, while the Morphing EnKF ensemble tracks the data successfully.

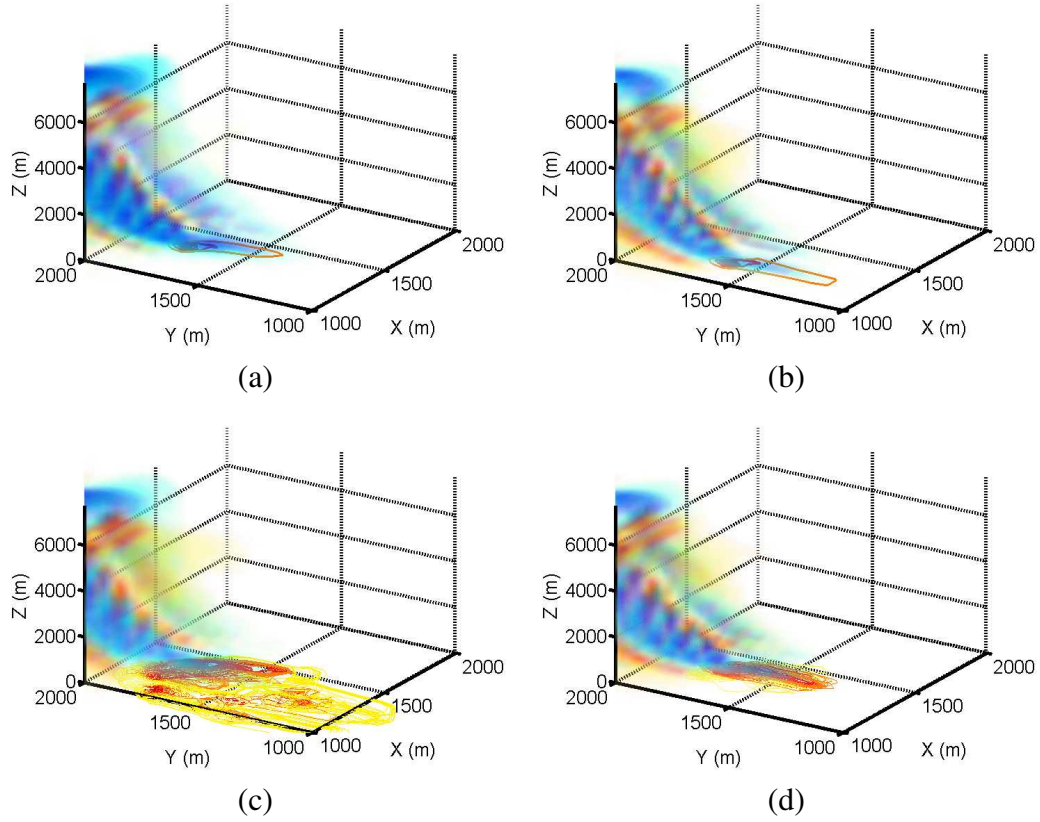


Fig. 7. The morphing EnKF applied to the fireline propagation model coupled with WRF. False color and contour on the horizontal plane is the output heat flux. The volume shading is the vorticity of the atmosphere where red and blue shades represent positive and negative vorticity, respectively. A contour plot of the heat flux due to the fire is shown on the x-y plane. The reference solution (a) is the simulated data. The initial ensemble was created by a random perturbation of the comparison solution (b), with the fire ignited at an intentionally incorrect location. The Standard ENKF (c) and the Morphing EnKF (d) were applied after 15 minutes. The ensembles have 25 members each. Shown are the mean vorticity and the superposition of the heat fluxes in ensemble members. The standard EnKF ensembles diverges from the data, while the Morphing EnKF ensemble tracks the data successfully.

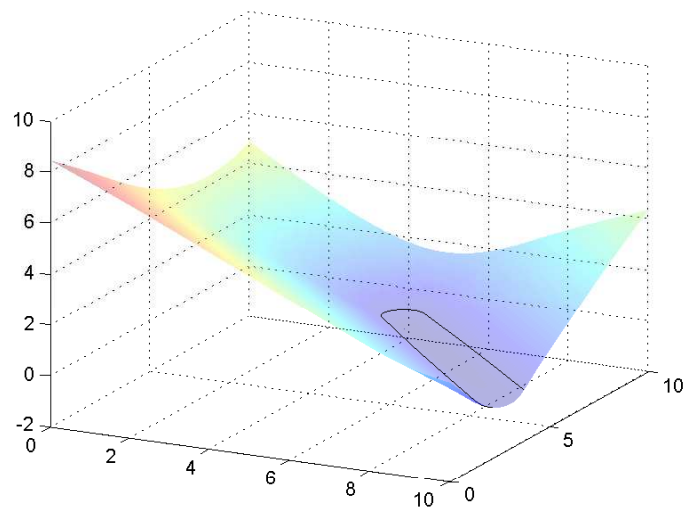


Fig. S1. The fireline and level function for a circular fire propagating in constant wind.